

Enhancing the efficiency of density functionals with an improved iso-orbital indicator

James W. Furness^{*} and Jianwei Sun[†]

Department of Physics and Engineering Physics, Tulane University, New Orleans, Louisiana 70118, USA

 (Received 25 May 2018; revised manuscript received 18 September 2018; published 30 January 2019)

The accuracy and efficiency of a density functional is dependent on the basic ingredients it uses and how the ingredients are built into the functional as a whole. An iso-orbital indicator based on the electron density, its gradients, and the kinetic energy density, has proven an essential dimensionless variable that allows density functionals to recognize and correctly treat various types of chemical bonding, both strong and weak. Density functionals constructed around the iso-orbital indicator usually require dense real-space grids for numerical implementation that deteriorate computational efficiency, with poor grid convergence compromising the improved accuracy. Here, an improved iso-orbital indicator is proposed based on the same ingredients that retains the capability to identify the same chemical bonds while significantly relieving the requirement of dense grids. Furthermore, the improved iso-orbital indicator gives an improved recognition for tail regions of electron densities and is divergence-free for the exchange-correlation potential. The improved iso-orbital indicator is therefore expected to be the prime choice for further density functional development.

DOI: [10.1103/PhysRevB.99.041119](https://doi.org/10.1103/PhysRevB.99.041119)

Density functional theory (DFT) is, in principle, exact for the ground-state energy and electron density of a system of electrons under a scalar external potential, conventionally solved through a set of Kohn-Sham (KS) auxiliary single-particle Schrödinger-like equations [1,2]. In practice, however, the exchange-correlation energy, an essential but usually small portion of the total energy, must be approximated as a functional of the electron density. The computational efficiency of this scheme and the accuracy of modern exchange-correlation approximations has resulted in DFT becoming one of the most widely used electronic structure theories and arguably the only practical method for high-throughput discovery of novel materials currently available.

Exchange-correlation approximations can be broadly categorized by the ingredients used into five levels of increasing nonlocality [3]. The accuracy of an approximation usually increases when more ingredients are included through increased flexibility though this enhancement is often accompanied by a deterioration of efficiency, especially when nonlocal information is included. It is therefore critical to understand the ingredients of common density functional approximations and how they can be utilized to increase the accuracy of a functional while maximizing the possible computational efficiency. As functionals of higher levels are usually developed based on functionals of lower levels, knowledge obtained for the ingredients and their combinations in lower-level functionals can be

transferred to the development of more complex functionals at higher levels.

The lowest three levels of efficient semilocal functionals include the local spin density approximation (LSDA) [2,4–8], the generalized gradient approximations (GGAs) [4,9–16], and meta-GGA [17–31]. LSDA uses only the electron density and recovers the uniform electron gas (UEG) limit. GGAs add the electron density gradient from which two standard dimensionless variables are constructed; $s = |\nabla n|/(2k_F n)$ with $k_F = (3\pi^2 n)^{1/3}$ relevant for exchange and $t_c = |\nabla n|/(2k_s n)$ with $k_s = \sqrt{4k_F/\pi}$ for correlation [32] measure the inhomogeneity of electron densities at the length scales of local Fermi wavelength $2\pi/k_F$ and Thomas screening length $1/k_s$, respectively. Commonly used meta-GGAs develop the functional to include more semilocal ingredients, commonly the kinetic energy density $\tau(\mathbf{r}) = 1/2 \sum_i^{\text{occ.}} |\nabla \phi_i(\mathbf{r})|^2$ where $\{\phi_i\}$ are KS orbitals. Based on their ingredients, the recently developed nonseparable gradient approximation (NGA) [33,34] and meta-NGA [25,35] can be included as levels 2 and 3, respectively.

The inclusion of τ in meta-GGAs naturally arises from the Taylor expansion of the exact spherically averaged exchange hole [36] and provides a simple and straightforward way to make a correlation functional exactly one-electron self-interaction free [19]. The flexibility due to the inclusion of τ improves the accuracy of meta-GGAs over GGAs, by either better fitting to experimental data empirically [18,23,28,31] or satisfying more exact constraints and appropriate norms nonempirically [21,24,26,29,30]. Early attempts [21,24] and the recent Tao-Mo functional [30] construct nonempirical meta-GGAs through an iso-orbital indicator defined as

$$z = \frac{\tau^{\text{vW}}}{\tau}, \quad (1)$$

where $\tau^{\text{vW}}(\mathbf{r}) = |\nabla n(\mathbf{r})|^2/8n(\mathbf{r})$ is the von Weizsäcker kinetic energy density that recovers τ in the single-orbital limit.

^{*}jfurness@tulane.edu

[†]jsun@tulane.edu

While z can identify single-orbital densities, $z = 1$, and slowly varying densities, $z \rightarrow 0$, it is unable to distinguish slowly varying densities from the noncovalent closed shell overlap densities important in intermediate-range van der Waals bonding [37]. A different indicator widely used in empirical constructions [23,28,35] is

$$t^{-1} = \frac{\tau}{\tau^{\text{UEG}}}, \quad (2)$$

where $\tau^{\text{UEG}} = (3/10)(3\pi^2)^{2/3}n^{5/3}$ is the kinetic energy density of uniform electron gas. While the t^{-1} indicator has been shown to differentiate covalent from noncovalent bonding, it cannot uniquely identify single-orbital regions for which $t^{-1} = 5s^2/3$. This is likely one of the major reasons for overfitting in the M06L meta-GGA and the resulting numerical stability problem of this functional [37]. t^{-1} is semi-infinite, $[0, \infty)$, and usually mapped to a finite domain via $w = (1 - t^{-1})/(1 + t^{-1}) = (\tau^{\text{UEG}} - \tau)/(\tau^{\text{UEG}} + \tau)$.

A further iso-orbital indicator has been constructed,

$$\alpha = \frac{\tau - \tau^{\text{vW}}}{\tau^{\text{UEG}}}, \quad (3)$$

which is able to uniquely identify single-orbital, slowly varying and noncovalent overlap densities as $\alpha = 0$, ≈ 1 and $\gg 1$, respectively. This indicator was included alongside z in earlier meta-GGA functionals [21,24] to enforce the correct fourth-order gradient expansion [38], though its importance for characterizing chemical environments was not fully recognized until later [37]. The α variable is directly related to the electron localization function (ELF) of Refs. [39,40] as $f_{\text{ELF}} = 1/(1 + \alpha^2)$ which has been used to give a rigorous topological classification of chemical bonding [41–43]. In addition, recent α -dependent functionals [29] have been found to effectively handle properties that have traditionally been challenging for semilocal functionals [44–48], including the intermediate-range van der Waals bonding [47] and metal-insulator transitions [48].

Despite the general success enjoyed by recent meta-GGA functionals for a wide range of systems [21,23,27–29,46–49], it has been observed that many meta-GGAs suffer numerical instabilities in self-consistent field (SCF) calculations [49,50], and have an unacceptably slow convergence with respect to the density of the numerical integration points [51,52]. The increased computational cost of dense numerical grids severely limits the usefulness of many meta-GGA functionals and restricts the complexity of systems to which they can be applied. Additionally, the uncertainty in overall grid convergence necessitates a time-consuming validation that calculated properties are properly converged in grid density, placing an undesirable burden of expertise on the user.

Within more advanced α -based functionals, it is understood that this numerical sensitivity originates from sharp oscillations in the exchange-correlation potential that are only properly dured by very fine grids [49], particularly in inter-shell regions where the local orbital overlap character can vary rapidly. Here we show that the rapid variations in the derivatives of α are largely responsible for these undesirable oscillations. Further, we propose a modified iso-orbital indicator quantity, termed β , from which new functionals can

TABLE I. Values of common iso-orbital indicators for typical chemical environments.

Region	t^{-1}	z	α	β
Single orbital	$5s^2/3$	1	0	0
Slowly varying density	≈ 1	≈ 0	≈ 1	$\approx \frac{1}{2}$
Noncovalent bonding	$\gg 1$	≈ 0	$\gg 1$	$\frac{1}{2} \ll \beta < 1$

be constructed that do not suffer this problem,

$$\beta(\mathbf{r}) = \frac{\tau(\mathbf{r}) - \tau^{\text{vW}}(\mathbf{r})}{\tau(\mathbf{r}) + \tau^{\text{UEG}}(\mathbf{r})} \quad (4)$$

$$= \alpha(\mathbf{r}) \left(\frac{\tau^{\text{UEG}}(\mathbf{r})}{\tau(\mathbf{r}) + \tau^{\text{UEG}}(\mathbf{r})} \right). \quad (5)$$

$$= \frac{\alpha(\mathbf{r})}{\alpha(\mathbf{r}) + \frac{5s(\mathbf{r})^2}{3} + 1}. \quad (6)$$

The β variable contains similar information about local orbital overlap environments to α while having smoother derivatives more easily amenable to evaluation on numerical grids. This allows local orbital overlap information to be used in functionals at the meta-GGA level and higher without suffering the numerical problems associated with analogous functions of the α variable.

The close relationship between the α and β variables can be shown by examining their limits in the three typical orbital overlap regions. Firstly, in single-orbital regions $\tau(\mathbf{r}) = \tau^{\text{vW}}(\mathbf{r})$ and $\alpha(\mathbf{r}) = \beta(\mathbf{r}) = 0$. This bound is important in exchange-correlation functional development, allowing the strong lower bound on exchange energy as well as correlation energy to be enforced for all spin-unpolarized single-orbital systems [29,53,54]. Secondly, in slowly varying densities $\tau^{\text{vW}}(\mathbf{r}) \rightarrow 0$ and $\tau(\mathbf{r}) \approx \tau^{\text{UEG}}(\mathbf{r})$, so $\alpha(\mathbf{r}) \approx 1$ and $\beta(\mathbf{r}) \approx 1/2$. Note α and β have different density gradient expansions in the slowly varying density limit (see Supplemental Material [55]). Finally, in noncovalent density overlap regions where $n(\mathbf{r}) \rightarrow 0$, $\tau^{\text{UEG}}(\mathbf{r}) \rightarrow 0$ as $n(\mathbf{r})^{5/3}$ while $\tau(\mathbf{r}) \rightarrow 0$ as $n(\mathbf{r})$ and $\tau^{\text{vW}}(\mathbf{r}) = 0$ at bond centers, and thus the denominator, $\tau^{\text{UEG}}(\mathbf{r})$, decays faster than the numerator, $\tau(\mathbf{r}) - \tau^{\text{vW}}(\mathbf{r})$, leading to $\alpha(\mathbf{r}) \rightarrow \infty$. Here $\beta(\mathbf{r})$ approaches 1 however, since both its numerator and denominator decay as $n(\mathbf{r})$. The relations between α , β , and other iso-orbital indicators are summarized in Table I.

This similarity between α and β in highlighting the local orbital overlap environment is shown graphically in Figs. 1(a) and 1(b) for the lithium and carbon atoms, respectively (see Supplemental Material [55] for a similar comparison for a wider range of atomic and small molecule systems). The lithium and carbon atoms were chosen as typically difficult systems with pronounced numerical sensitivity for density functionals. The similar intershell peak behavior is clearly visible for both variables as a rise away from single-orbital-like values of the $1s$ core. The difference between α and β is seen in the tail region of the carbon atom for the majority spin electrons, where α diverges upward while β decays slowly toward 0. For the minority spin, both α and β approach 0 in the tail region. In general, β consistently indicates the tail regions of all densities with 0 as $\tau^{\text{vW}}(\mathbf{r})$ is the leading order of $\tau(\mathbf{r})$

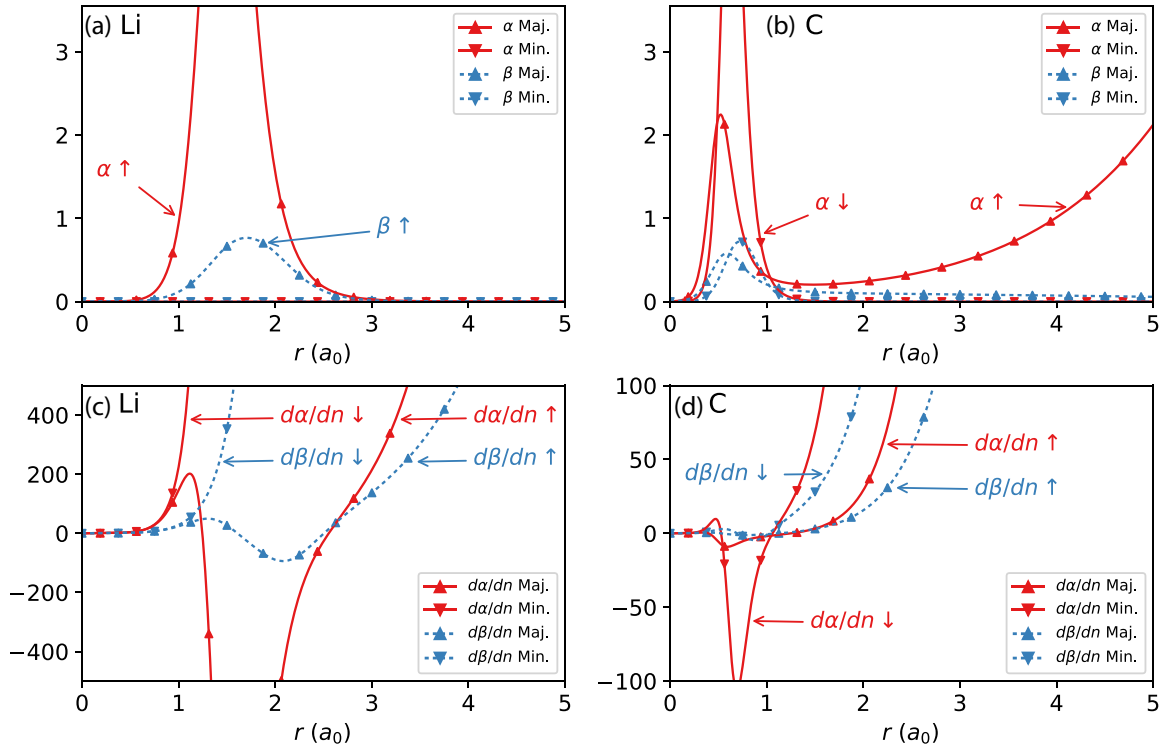


FIG. 1. Radial plots of $\alpha(r)$ and $\beta(r)$ functions and their density derivatives for the lithium and carbon atoms. The α (solid red) and β (dashed blue) functions and density derivatives are plotted for the majority (Maj., \blacktriangle) and minority (Min., \blacktriangledown) spin from self-consistent Perdew-Burke-Ernzerhof (PBE) [11] densities. Radial distances are in units of Bohr.

there, and identifies tail regions completely when combined with the dimensionless reduced density gradient, s , that is divergent. This is impossible for α since $\alpha(r) = 0$ for the tail regions of single-orbital systems and $\alpha \rightarrow \infty$ otherwise. This shortcoming results in α -based meta-GGAs biasing tail regions toward a uniform electron gas description, rather than that of a single orbital [56].

The benefit of β over α for functional development is most clearly seen in the derivatives with respect to density, exemplified in Figs. 1(c) and 1(d) for the lithium and carbon atoms, respectively. The derivative of β with respect to density does not show the same rapid variation as that of α in intershell and valence regions where density is significant. Similar behavior is observed for $|\nabla n|$ and τ derivatives, as noted for α in Ref. [49] and in the more complex molecular systems presented in the Supplemental Material.

The much better behaved derivatives of β over those of α remedy the numerical problems observed in α -dependent meta-GGA functionals. To validate this, we modify the existing *meta-GGA made simple 2* (MS2) functional [57] by substituting 2β in place of α within the exchange enhancement factor $F_x(s, \alpha)$, defined by

$$E_x^{\text{meta-GGA}}[n] = \int e_x^{\text{UEG}}(n) F_x^{\text{meta-GGA}}(s, \alpha) d\mathbf{r}, \quad (7)$$

where $e_x^{\text{UEG}}(n) = -3(3\pi^2)^{1/3} n^{4/3} / 4\pi$ is the exchange energy density of uniform electron gas. MS2 has a simple construction of $F_x^{\text{MS2}}(s, \alpha) = F_x^1(s) + f_x^{\text{MS2}}(\alpha)[F_x^0(s) - F_x^1(s)]$ with

$$f_x^{\text{MS2}}(\alpha) = \frac{(1 - \alpha^2)^3}{1 + \alpha^3 + b\alpha^6} \quad (8)$$

that interpolates between $F_x^0(s)$, a GGA for single-orbital systems ($\alpha = 0$), and $F_x^1(s)$, a GGA for slowly varying densities ($\alpha \approx 1$), and extrapolates to ($\alpha \gg 1$) for noncovalent bonds.

This functional was chosen for the relatively simple construction and well reported numerical instabilities [49]. Modification of the simple exchange enhancement factor for β dependence was trivial by replacing α with 2β to guarantee the interpolation between $F_x^0(s)$ for single-orbital systems ($2\beta = \alpha = 0$) and $F_x^1(s)$ for slowly varying densities ($2\beta \approx \alpha \approx 1$). The resulting β -modified meta-GGA functional is termed MS2 β . The parameter b is determined such that $f_x^{\text{MS2}\beta}(\beta = 1) = f_x^{\text{MS2}}(\alpha \rightarrow \infty)$ for noncovalent bonds. These minor adjustments to the balances between internal parameters to preserve exact constraints obeyed by the parent functional are summarized in Table II and detailed in the Supplemental Material [55]. MS2 β was implemented into the TURBOMOLE package [58] using the XCFUN library [59] to automatically evaluate functional derivatives. We present MS2 β simply as

TABLE II. Parameters for the MS2 and MS2 β functionals. The notation of Ref. [57] is followed, with constants $k_0 = 0.174$ and $\mu_{\text{GE}} = 10/81$.^a

Functional	κ	b	c
MS2	0.504	4.0	0.14607 ^a
MS2 β	0.504	$(27b^{\text{MS2}} - 9)/64$	0.14607

^aThe original publication of MS2 [37] gives $c = 0.14601$. We find this gives a small error (on the order of μE_h) in the exchange energy of the hydrogen atom that is corrected using $c = 0.14607$. We note however, that this change has negligible impact on MS2 predicted atomization energies and barrier heights.

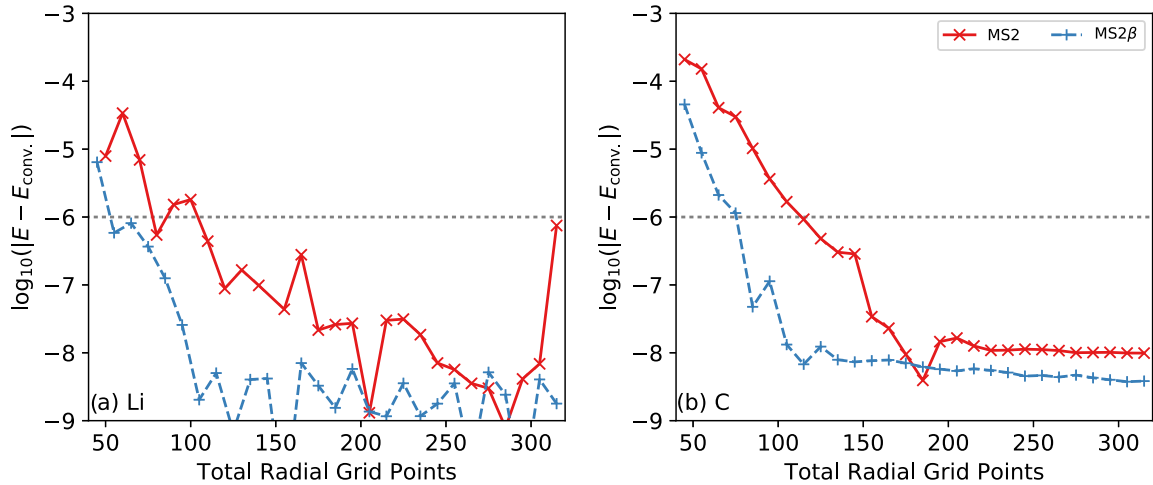


FIG. 2. Convergence behavior with respect to numerical grid density of conventional and the β -modified *meta-GGA made simple 2* (MS2) functional [57] for (a) lithium and (b) carbon atoms. Difference in self-consistent atomic total energy relative to the total energy from a converged grid of 520 points ($E_{\text{conv.}}$) for the MS2 (red, \times) and MS2 β (blue, dashed, +) functionals using the aug-cc-pVQZ basis set [60]. An acceptable convergence is assumed when difference remains below the SCF convergence tolerance of $1\mu E_h$ (dotted line).

a convenient means for preliminary investigation of the β variable rather than as a viable general functional.

The grid convergence of the MS2 and MS2 β functionals is shown in Fig. 2 as a plot of the difference in self-consistent electronic energy relative to the same calculation using a very fine benchmark grid, as a function of grid point density, for the carbon and lithium atoms. In both cases the β -modified functional shows a convergence in total energy at lower grid density than the parent α functional, indicated by the difference to the benchmark grid energy remaining below the SCF convergence threshold of $1\mu E_h$.

As previously noted, the sensitivity of α -dependent functionals to numerical integration grid point density is understood as an effect of rapid oscillations in the exchange-correlation potential, \hat{v}_{xc} , expressed in the generalized Kohn-Sham scheme [49,61,62] as

$$\int \varphi_p \hat{v}_{xc} \varphi_q d\mathbf{r} = \int \varphi_p \frac{\partial e_{xc}}{\partial n} \varphi_q d\mathbf{r} + \int \frac{\partial e_{xc}}{\partial \nabla n} \cdot \nabla (\varphi_p \varphi_q) d\mathbf{r} + \frac{1}{2} \int \nabla \varphi_p \cdot \left(\frac{\partial e_{xc}}{\partial \tau} \right) \nabla \varphi_q d\mathbf{r}. \quad (9)$$

Here, e_{xc} is the exchange-correlation energy density of a meta-GGA functional. Hence, functionals showing sharp oscillations in functional derivatives will show sharp variations in exchange-correlation potential that are challenging to dure in numerical integration schemes. By modifying meta-GGA functionals to use the β indicator in place of α , oscillations in functional derivatives are minimized and the resulting exchange-correlation potential is smoothed, as exemplified by MS2 and MS2 β which have the same exchange enhancement factor form in terms of α or 2β dependence. We can therefore understand the reduced grid sensitivity of the β -modified functional as a consequence of smoother functional derivatives in the intershell and valence regions producing smoother exchange-correlation potentials that can be more easily dured by numerical integration grids.

The divergences of derivatives at tails seen in Figs 1(c) and 1(d) are not problematic for the exchange-correlation potential of analytic β -dependent meta-GGAs because $e_x^{\text{UEG}}(n)$ decays faster than the divergence of β derivatives there. However, the divergences of α derivatives at tails are much stronger than those of β , also seen in Figs 1(c) and 1(d), and can cause problems for the exchange-correlation potential of α -dependent meta-GGAs. At the tail regions, τ decays as n , while τ^{UEG} decays more quickly as $n^{5/3}$, so the derivative of α with respect to, for example, τ diverges as $n^{-5/3}$, faster than the decay of $e_x^{\text{UEG}}(n)$ which is proportional to $n^{4/3}$. This can lead to divergences of exchange-correlation potential for α -dependent meta-GGAs as long as the derivative of $F_x^{\text{meta-GGA}}(s, \alpha)$ with respect to α is nonzero at the tail. Such nonzero values are encountered in the *meta-GGA made very simple* (MVS) [54] and SCAN [29] meta-GGAs at the tail regions of single-orbital systems [63]. This behavior is avoided in β as the decay of both the numerator and denominator of β is determined by τ as decaying with n .

The potential divergence of exchange-correlation potential at tail regions resulting from the strong divergence of α derivatives is undesirable and problematic especially for the construction of pseudopotentials from isolated atoms, acting as a hitherto unrecognized additional restriction on α -dependent functional design. This restriction was not previously noticed and is not obeyed by the MVS [54] and SCAN [29] functionals, though it is fortuitously obeyed by MS2. This restriction is not necessary in β -dependent functionals however, as the asymptotic behavior of β is properly controlled and thus β offers simplicity and greater flexibility in functional design compared to the α indicator.

To show that the MS2 β functional retains the ability to effectively distinguish different chemical environments we first test it against the small data sets of atomization energies (AE6) and barrier heights (BH6) [66,67], the results for which are shown in Table III, with DFT grid convergence behaviors shown in the Supplemental Material [55]. For these small datasets the accuracy of the β -modified functional is

TABLE III. Mean error (ME) and mean absolute error (MAE) in kcal mol⁻¹ for the small test sets of atomization energy (AE6) and reaction barrier height (BH6) for the PBE [11], MS2, and MS2 β functionals. All calculations were performed fully self-consistently with the 6-311++G(3df,3pd) basis set [64,65] on a dense numerical grid (TURBOMOLE level 7).

	PBE	MS2	MS2 β
AE6 (ME)	12.47	-0.78	3.95
AE6 (MAE)	15.58	4.40	6.10
BH6 (ME)	-9.67	-5.79	-6.32
BH6 (MAE)	9.67	5.79	6.32

only slightly reduced compared to the original and remains significantly better than that of the PBE GGA.

The different behavior of the α and β variables is most pronounced in regions of noncovalent density overlap where $\alpha(\mathbf{r}) \gg 1.0$ and β is in the region $0.5 \ll \beta(\mathbf{r}) < 1.0$. This difference is most clearly examined in the Ar₂ dissociation curve, for which it has been shown meta-GGA functionals can be accurate around equilibrium [29,47,57]. The dissociation curves for Ar₂ are shown in Fig. 3 for both the conventional and β -modified MS2 functionals with benchmark data included from Ref. [68] for comparison. In contrast to the small test sets, MS2 β closely matches the performance of the original MS2 functional across the whole of the binding curve showing far greater accuracy than that of the PBE GGA. The performance of MS2 β for AE6, BH6, and the Ar₂ diatomic in comparison to those of MS2 and PBE clearly demonstrates its capability to recognize different chemical environments. As the MS2 meta-GGA is a simple density functional that only satisfies a subset of exact constraints relevant to meta-GGAs [26,29,37], a simple substitution of β for α cannot guarantee the accuracy of the original MS2 functional as seen in the AE6 and BH6 data sets.

In conclusion, we have identified that sharp oscillations in the functional derivatives of the commonly employed dimensionless variable α can cause numerical sensitivities in meta-GGA calculations. We have addressed these sensitivities by constructing a related dimensionless variable, β , which imparts similar information about the local orbital overlap environment while having smoother functional derivatives. The enhanced numerical stability, improved recognition of tail regions, and freedom from restrictions on exchange-correlation potential presented by β are an appealing opportunity for enhancing the performance of future functionals for both the meta-GGA level and higher level fully nonlocal functionals.

We have used the simple MS2 meta-GGA functional as a proof of concept by substituting 2β for α in the functional

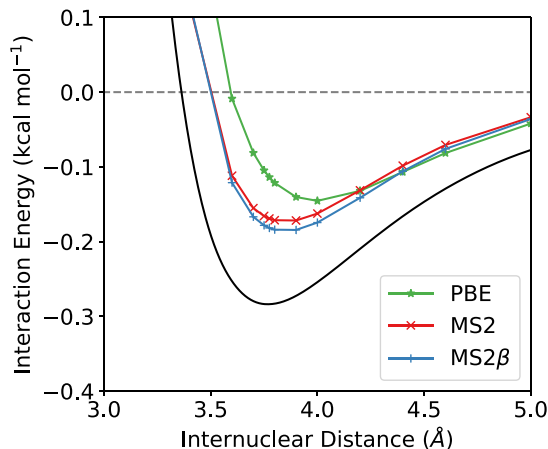


FIG. 3. Dissociation curve of the argon dimer. Calculated using PBE (green, \star), MS2 (red, \times), and MS2 β (blue, $+$) functionals. Calculations performed self-consistently using the aug-cc-pV5Z basis set and a very fine numerical grid (grid 7 of the TURBOMOLE program). A benchmark curve (black) is included from Ref. [68].

with minimal adjustment of internal parameters. We find improved numerical performance in all cases, with the new functional giving converged properties from much coarser integration grids than the original MS2 functional. Testing MS2 β against MS2 and PBE on small molecules clearly shows the capability of β to recognize different chemical environments at the functional performance level, and suggests the need for embedding β into more sophisticated density functional constructions. We are optimistic that wholly novel functionals utilizing the β iso-orbital indicator can provide ever greater accuracy and utility for the wider DFT community.

We thank Jefferson Bates for his invaluable technical advice in running and modifying the TURBOMOLE package. We also thank John Perdew, Adrienn Ruzsinszky, Mark Pederson, Weitao Yang, Arun Bansil, Samuel Trickey, Donald Truhlar, Susi Lehtola, Albert Bartok-Partay, Natalie Holzwarth, and Yosuke Kanai for their fruitful discussions around the ideas presented here. We acknowledge Natalie Holzwarth for pointing out the divergence in SCAN exchange-correlation potential for the hydrogen atom. The work was supported by the start-up funding from Tulane University, and by the U.S. DOE, Office of Science, Basic Energy Sciences Grant No. DE-SC0019350 (core research). Calculations were carried out on the Cypress cluster at Tulane University, and we thank Dr. Hoang Tran, Dr. Carl Baribault, and Dr. Hideki Fujioka for their computational support.

- [1] P. Hohenberg and W. Kohn, *Phys. Rev.* **136**, B864 (1964).
 [2] W. Kohn and L. J. Sham, *Phys. Rev.* **140**, A1133 (1965).
 [3] J. P. Perdew and K. Schmidt, in *Density Functional Theory and its Application to Materials*, AIP Conf. Proc. No. 577 (AIP, Melville, NY, 2001), p. 1.
 [4] S.-K. Ma and K. A. Brueckner, *Phys. Rev.* **165**, 18 (1968).

- [5] U. Von Barth and L. Hedin, *J. Phys. C* **5**, 1629 (1972).
 [6] J. P. Perdew and A. Zunger, *Phys. Rev. B* **23**, 5048 (1981).
 [7] J. P. Perdew and Y. Wang, *Phys. Rev. B* **45**, 13244 (1992).
 [8] J. Sun, J. P. Perdew, and M. Seidl, *Phys. Rev. B* **81**, 085123 (2010).
 [9] A. D. Becke, *Phys. Rev. A* **38**, 3098 (1988).

- [10] J. P. Perdew, J. A. Chevary, S. H. Vosko, K. A. Jackson, M. R. Pederson, D. J. Singh, and C. Fiolhais, *Phys. Rev. B* **46**, 6671 (1992).
- [11] J. P. Perdew, K. Burke, and M. Ernzerhof, *Phys. Rev. Lett.* **77**, 3865 (1996).
- [12] T. W. Keal and D. J. Tozer, *J. Chem. Phys.* **121**, 5654 (2004).
- [13] R. Armiento and A. E. Mattsson, *Phys. Rev. B* **72**, 085108 (2005).
- [14] J. P. Perdew, A. Ruzsinszky, G. I. Csonka, O. A. Vydrov, G. E. Scuseria, L. A. Constantin, X. Zhou, and K. Burke, *Phys. Rev. Lett.* **100**, 136406 (2008).
- [15] L. A. Constantin, E. Fabiano, S. Laricchia, and F. Della Sala, *Phys. Rev. Lett.* **106**, 186406 (2011).
- [16] A. Vela, J. C. Pacheco-kato, J. L. Gázquez, J. M. Campo, and S. B. Trickey, *J. Chem. Phys.* **136**, 144115 (2012).
- [17] A. D. Becke and M. R. Roussel, *Phys. Rev. A* **39**, 3761 (1989).
- [18] T. Van Voorhis and G. E. Scuseria, *J. Chem. Phys.* **109**, 400 (1998).
- [19] A. D. Becke, *J. Chem. Phys.* **109**, 2092 (1998).
- [20] J. P. Perdew, S. Kurth, A. Zupan, and P. Blaha, *Phys. Rev. Lett.* **82**, 2544 (1999).
- [21] J. Tao, J. P. Perdew, V. N. Staroverov, and G. E. Scuseria, *Phys. Rev. Lett.* **91**, 146401 (2003).
- [22] A. D. Becke, *J. Chem. Phys.* **119**, 2972 (2003).
- [23] Y. Zhao and D. G. Truhlar, *J. Chem. Phys.* **125**, 194101 (2006).
- [24] J. P. Perdew, A. Ruzsinszky, G. I. Csonka, L. A. Constantin, and J. Sun, *Phys. Rev. Lett.* **103**, 026403 (2009).
- [25] H. S. Yu, X. He, and D. G. Truhlar, *J. Chem. Theory Comput.* **12**, 1280 (2016).
- [26] J. Sun, B. Xiao, and A. Ruzsinszky, *J. Chem. Phys.* **137**, 051101 (2012).
- [27] J. M. Del Campo, J. L. Gázquez, S. B. Trickey, and A. Vela, *Chem. Phys. Lett.* **543**, 179 (2012).
- [28] N. Mardirossian and M. Head-Gordon, *J. Chem. Phys.* **142**, 074111 (2015).
- [29] J. Sun, A. Ruzsinszky, and J. P. Perdew, *Phys. Rev. Lett.* **115**, 036402 (2015).
- [30] J. Tao and Y. Mo, *Phys. Rev. Lett.* **117**, 073001 (2016).
- [31] Y. Wang, X. Jin, H. S. Yu, D. G. Truhlar, and X. He, *Proc. Natl. Acad. Sci.* **114**, 8487 (2017).
- [32] J. P. Perdew, L. A. Constantin, E. Sagvolden, and K. Burke, *Phys. Rev. Lett.* **97**, 223002 (2006).
- [33] R. Peverati and D. G. Truhlar, *J. Chem. Theory Comput.* **8**, 2310 (2012).
- [34] H. S. Yu, W. Zhang, P. Verma, X. He, and D. G. Truhlar, *Phys. Chem. Chem. Phys.* **17**, 12146 (2015).
- [35] R. Peverati and D. G. Truhlar, *Phys. Chem. Chem. Phys.* **14**, 13171 (2012).
- [36] A. D. Becke, *Int. J. Quantum Chem.* **23**, 1915 (1983).
- [37] J. Sun, B. Xiao, Y. Fang, R. Haunschuld, P. Hao, A. Ruzsinszky, G. I. Csonka, G. E. Scuseria, and J. P. Perdew, *Phys. Rev. Lett.* **111**, 106401 (2013).
- [38] P. S. Svendsen and U. von Barth, *Phys. Rev. B* **54**, 17402 (1996).
- [39] A. D. Becke and K. E. Edgecombe, *J. Chem. Phys.* **92**, 5397 (1990).
- [40] B. Silvi and A. Savin, *Nature (London)* **371**, 683 (1994).
- [41] A. Savin, B. Silvi, and F. Colonna, *Can. J. Chem.* **74**, 1088 (1996).
- [42] A. Savin, R. Nesper, S. Wengert, and T. F. Fässler, *Angew. Chem., Int. Ed. Engl.* **36**, 1808 (1997).
- [43] S. Noury, F. Colonna, A. Savin, and B. Silvi, *J. Mol. Struct.* **450**, 59 (1998).
- [44] A. Paul, J. Sun, J. P. Perdew, and U. V. Waghmare, *Phys. Rev. B* **95**, 054111 (2017).
- [45] Y. Zhang, J. Sun, J. P. Perdew, and X. Wu, *Phys. Rev. B* **96**, 035143 (2017).
- [46] Y. Zhang, D. A. Kitchaev, J. Yang, T. Chen, S. T. Dacek, R. A. Sarmiento-Pérez, M. A. L. Marques, H. Peng, G. Ceder, J. P. Perdew, and J. Sun, *npj Comput. Mater.* **4**, 9 (2018).
- [47] J. Sun, R. C. Remsing, Y. Zhang, Z. Sun, A. Ruzsinszky, H. Peng, Z. Yang, A. Paul, U. Waghmare, X. Wu, M. L. Klein, and J. P. Perdew, *Nat. Chem.* **8**, 831 (2016).
- [48] J. W. Furness, Y. Zhang, C. Lane, I. G. Buda, B. Barbiellini, R. S. Markiewicz, A. Bansil, and J. Sun, *Commun. Phys.* **1**, 11 (2018).
- [49] Z.-h. Yang, H. Peng, J. Sun, and J. P. Perdew, *Phys. Rev. B* **93**, 205205 (2016).
- [50] E. R. Johnson, A. D. Becke, C. D. Sherrill, and G. A. Dilabio, *J. Chem. Phys.* **131**, 034111 (2009).
- [51] Y. Yao and Y. Kanai, *J. Chem. Phys.* **146**, 224105 (2017).
- [52] N. Mardirossian and M. Head-Gordon, *Mol. Phys.* **115**, 2315 (2017).
- [53] J. P. Perdew, A. Ruzsinszky, J. Sun, and K. Burke, *J. Chem. Phys.* **140**, 18A533 (2014).
- [54] J. Sun, J. P. Perdew, and A. Ruzsinszky, *Proc. Natl. Acad. Sci. USA* **112**, 685 (2015).
- [55] See Supplemental Material at <http://link.aps.org/supplemental/10.1103/PhysRevB.99.041119> for further plots of α , β , and their derivatives for varied chemical systems; derivation of the MS2 β functional; total energies of neon and argon for MS2 and MS2 β ; grid convergence of small molecular test sets; and a brief comment on current sensitive β for strong magnetic fields.
- [56] J. Hermann and A. Tkatchenko, *J. Chem. Theory Comput.* **14**, 1361 (2018).
- [57] J. Sun, R. Haunschuld, B. Xiao, I. W. Bulik, G. E. Scuseria, and J. P. Perdew, *J. Chem. Phys.* **138**, 044113 (2013).
- [58] TURBOMOLE V7.2 2018, a development of University of Karlsruhe and Forschungszentrum Karlsruhe GmbH, 1989-2007, TURBOMOLE GmbH, since 2007; available from <http://www.turbomole.com>.
- [59] U. Ekström, L. Visscher, R. Bast, and A. J. Thorvaldsen, *J. Chem. Theory Comput.* **6**, 1971 (2010).
- [60] T. H. Dunning, *J. Chem. Phys.* **90**, 1007 (1989).
- [61] R. Neumann, R. H. Nobes, and N. C. Handy, *Mol. Phys.* **87**, 1 (1996).
- [62] A. Seidl, A. Görling, P. Vogl, J. A. Majewski, and M. Levy, *Phys. Rev. B* **53**, 3764 (1996).
- [63] N. Holzwarth (private communication).
- [64] T. Clark, J. Chandrasekhar, G. W. Spitznagel, and P. V. R. Schleyer, *J. Comput. Chem.* **4**, 294 (1983).
- [65] M. J. Frisch, J. A. Pople, and J. S. Binkley, *J. Chem. Phys.* **80**, 3265 (1984).
- [66] B. J. Lynch and D. G. Truhlar, *J. Phys. Chem. A* **107**, 8996 (2003).
- [67] R. Haunschuld and W. Klopper, *Theor. Chem. Acc.* **131**, 1112 (2012).
- [68] K. Patkowski, G. Murdachaew, C. M. Fou, and K. Szalewicz, *Mol. Phys.* **103**, 2031 (2005).